

Cooperative and anticooperative binding to a ribozyme

(pyrene/ribonucleic acid/cooperativity/kinetics/thermodynamics)

PHILIP C. BEVILACQUA*, KENNETH A. JOHNSON†, AND DOUGLAS H. TURNER*‡

*Department of Chemistry, University of Rochester, Rochester, NY 14627; and †Department of Molecular and Cell Biology, Pennsylvania State University, Altoona Laboratory, University Park, PA 16802

Communicated by I. Tinoco, Jr., June 1, 1993

ABSTRACT The effects of guanosine 5'-monophosphate and 2'-deoxyguanosine 5'-monophosphate on the thermodynamics and kinetics of pyrene-labeled 5' exon mimic (pyCUCU) binding to the catalytic RNA (ribozyme) from *Tetrahymena thermophila* have been determined by fluorescence titration and kinetics experiments at 15°C. pyCUCU binding to L-21 *Sca* I-truncated ribozyme is weaker by a factor of 5 in the presence of saturating guanosine 5'-monophosphate, whereas it is 4-fold stronger in the presence of saturating 2'-deoxyguanosine 5'-monophosphate. Results from kinetics experiments suggest that anticooperative effects in the presence of guanosine 5'-monophosphate arise primarily from slower formation of tertiary contacts between the catalytic core of the ribozyme and the P1 duplex formed by pyCUCU and GGAGGG of the ribozyme. Conversely, cooperative effects in the presence of 2'-deoxyguanosine 5'-monophosphate arise primarily from slower disruption of tertiary contacts between the catalytic core of the ribozyme and the P1 duplex. Additional experiments suggest that these cooperative and anticooperative effects are not a function of the pyrene label, are not caused by a salt effect, and are not specific to one renaturation procedure for the ribozyme.

Regulation of enzyme activity is often mediated by cooperative and anticooperative interactions among substrates. Coupling of substrate binding has been the subject of many theoretical investigations (1–4). Substrate interactions allow enzymes to respond to changes in their environment (5–8). Indeed, the activity of several enzymes is regulated by the binding of a single nucleotide cofactor (9–12). The L-21 *Sca* I-truncated catalytic RNA (ribozyme), designated "L-21 *Sca* I," derived from the self-splicing LSU intron of *Tetrahymena thermophila* has two substrate-binding sites: one for the nucleotide guanosine and its 5'-phosphate derivatives and one for 5'-splice-site mimics, including CUCU (13, 33), opening the possibility for heterotropic substrate interactions. In addition, the G-binding site can also accommodate dG, a competitive inhibitor of G (14).

Recent experiments on mutants of L-21 *Sca* I (15) and stopped-flow experiments with fluorescent pyrene derivatives of 5' exon mimics (16, 17) established that 5'-exon mimics bind to L-21 *Sca* I in two steps. The first step is base pairing to GGAGGG (the internal guide sequence) to form the P1 pairing (18, 19), and the second step is formation of tertiary contacts between P1 and the catalytic core of the ribozyme (Fig. 1). At least some of these tertiary contacts involve specific 2'-OH groups of the 5'-exon mimic at the underlined positions: CUCU (20, 21).

We report here that the nucleotide cofactor guanosine 5'-monophosphate (pG) causes pyrene-labeled CUCU (pyCUCU) binding to L-21 *Sca* I to be weaker by a factor of 5 (+0.9 kcal/mol at 15°C), whereas the inhibitor 2'-deoxy-

guanosine 5'-monophosphate (pdG) causes pyCUCU binding to be 4-fold stronger (–0.8 kcal/mol at 15°C) (Fig. 1). Coupling between binding of pyCUCU and pG or pdG arises primarily from effects of the G substrate on the second step of pyCUCU binding—formation and disruption of tertiary contacts (Fig. 1). These cooperative and anticooperative effects are of similar magnitude to those observed with proteins (22), suggesting potential roles for cooperativity in regulation of splicing and in ordering the kinetic steps of splicing.

MATERIALS AND METHODS

All experiments are at 15°C and, except where noted, in 5.0 mM MgCl₂/135 mM NaCl/50 mM Hepes (25 mM Na⁺) at pH 7.4. Except where noted, L-21 *Sca* I was prepared and renatured as described (13, 21). Pyrene-modified oligonucleotides were synthesized chemically (17). Cofactors pG (Fluka), pdG, adenosine 5'-monophosphate (pA), and 2'-deoxyadenosine 5'-monophosphate (pdA) (Sigma) were used at concentrations of 5 or 15 mM or both.

Fluorescence Binding Titrations. Titrations were performed on a Perkin-Elmer MPF-44A fluorimeter with excitation at 329 nm and emission at 397 nm. The concentration of pyCUCU was always at least slightly in excess over the concentration of L-21 *Sca* I. The total concentration of L-21 *Sca* I was held constant at 40 nM, 50 nM, and 1.0 μM for titrations with no cofactor, 15 mM pdG, and 15 mM pG, respectively. To obtain the K_d for pyCUCU binding to L-21 *Sca* I, the fraction of maximal fluorescence increase (f) with [pyCUCU] is directly fit by nonlinear least-squares to the quadratic equation, $f = 0.5 ([L-21 Sca I]_0 + [pyCUCU]_0 + K_d) - \{0.25 ([L-21 Sca I]_0 + [pyCUCU]_0 + K_d)^2 - [L-21 Sca I]_0 [pyCUCU]_0\}^{1/2} / [L-21 Sca I]_0$, where []₀ represents initial concentration.

Kinetics Experiments. The change in fluorescence with time fit single exponentials for all kinetics experiments reported. Manual mixing experiments were performed on a Perkin-Elmer MPF-44A fluorimeter with excitation at 329 nm and emission at 397 nm. Rapid-mixing, stopped-flow experiments were as described (16, 23). The concentration of pyCUCU in kinetics experiments was in excess of L-21 *Sca* I to maintain pseudo-first-order conditions. Kinetic data with 5 and 15 mM pdG, 15 mM pA, 15 mM pdA, or 180 mM NaCl (no cofactor) were obtained with 50 nM L-21 *Sca* I (final concentration) by either manual mixing or stopped-flow. Kinetic data with no cofactor (16) and 15 mM pG were obtained with 40 nM and 500 nM L-21 *Sca* I (final concentrations), respectively, by stopped-flow.

Pulse-chase experiments with no cofactor and either 135 or 180 mM NaCl, 5 and 15 mM pdG, 15 mM pA, and 15 mM pdA were conducted by incubating 80 μl of 100 nM L-21 *Sca* I and

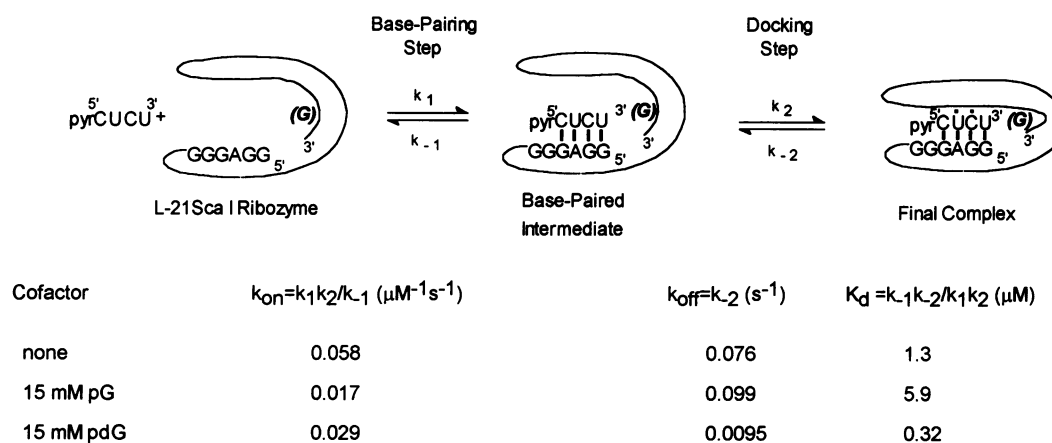


FIG. 1. Schematic of pyCUCU (pyrCUCU) binding to L-21 *Sca* I as described in text. The G-binding site is depicted by "(G)" and is empty or filled with pG or pdG depending on the experiment. Known base pairing is indicated by bold lines (18, 19), and known tertiary hydrogen bonds involving 2'-OH groups of pyCUCU are indicated by bold dots (20, 21).

1 μM pyCUCU in the appropriate buffer and cofactor for at least 10 min at 15°C (the pulse). Then 80 μl of 10 μM CUCU in the appropriate buffer and the cofactor were added either manually or by stopped-flow (the chase). Pulse-chase experiments with 15 mM pG were conducted by incubating 30 μl of 500 nM L-21 *Sca* I and 5 μM pyCUCU in buffer with 15 mM pG for at least 10 min at 15°C (the pulse). Then 30 μl of 50 μM CUCU in buffer with 15 mM pG was added by stopped-flow (the chase).

Pulse-chase experiments with pyCCUCU were conducted by incubating 80 μl of 100 nM L-21 *Sca* I and 100 nM pyCCUCU in buffer with the appropriate cofactor, if any, for at least 10 min at 15°C (the pulse). Then 80 μl of 10 μM CCUCU in buffer with the appropriate cofactor was added manually (the chase).

Reversed pulse-chase experiments with no cofactor or 15 mM pdG were conducted by incubating 80 μl of 100 nM L-21 *Sca* I and 1 μM CUCU in buffer with no cofactor or 15 mM pdG for at least 10 min at 15°C (the pulse). Then 80 μl of 10 μM pyCUCU in buffer with no cofactor or 15 mM pdG was added manually (the chase). Reversed pulse-chase experiments with 15 mM pG were conducted by incubating 30 μl of 500 nM L-21 *Sca* I and 5 μM CUCU in buffer with 15 mM pG for at least 10 min at 15°C (the pulse). Then 30 μl of 50 μM pyCUCU in buffer with 15 mM pG was added by stopped-flow (the chase). Since pyCUCU has a fluorescence increase of ≈ 20 -fold upon binding to L-21 *Sca* I, these experiments had a good signal-to-noise ratio, thus providing k_{-2} for unlabeled CUCU.

Alternate Renaturation Experiments. In selected experiments, to test the effect of renaturation on binding, L-21 *Sca* I was renatured by heating the ribozyme to 50°C for 10 min in the buffer described above, incubating at 15°C for 10 min in buffer, and incubating at 15°C for at least another 10 min in buffer with the appropriate cofactor, if any. Pulse-chase experiments were then performed as described above.

RESULTS

Fluorescence Titrations. Binding of pyCUCU to L-21 *Sca* I in the presence or absence of a G-like substrate was assessed by fluorescence titrations. Titrations of pyCUCU binding to L-21 *Sca* I in the presence of either 15 mM pG or 15 mM pdG led to binding of pyCUCU that was respectively weaker (+0.8 kcal/mol) and stronger (-0.8 kcal/mol) by factors of 4 (Fig. 2 and Tables 1 and 2). Equilibrium dialysis experiments at 15°C in the presence of saturating d(CT)₃ indicate that the K_d for pG binding to L-21 *Sca* I is 1.5 mM (24). A similar K_d is expected for pdG since pdG binds slightly more tightly than

pG at 5°C (24). Thus, the G-binding site is $\approx 90\%$ saturated in these experiments.

Kinetics Experiments for pyCUCU and L-21 *Sca* I with pG and pdG. To assess whether the binding effects are due to the "on" rate for capture of substrate into the catalytic core [k_{on} ($= k_1k_2/k_{-1}$ for pyCUCU)] or the rate of undocking of the P1 duplex from the catalytic core [k_{off} ($= k_{-2}$ for pyCUCU)], kinetics experiments were performed with pyCUCU (Fig. 3). The slope of a plot in Fig. 3 gives k_1k_2/k_{-1} , the intercept gives k_{-2} , and the ratio of the intercept to the slope gives K_d (16). The ratios of intercept to slope for pyCUCU binding to L-21 *Sca* I indicate that pG and pdG weaken and strengthen binding by factors of 5 (+0.9 kcal/mol) and 4 (-0.8 kcal/mol), respectively, in agreement with titration experiments in Fig. 2 (Table 2). The rate constants indicate that pyCUCU binds more weakly in the presence of pG primarily because of an "on" rate (k_1k_2/k_{-1}) that is slower by a factor of 3.5, whereas pyCUCU binds more strongly in the presence of pdG primarily because of a slower rate of dissociation by a factor of 8 of tertiary contacts, k_{-2} (Table 1). In fact, pdG also leads to a 50% slower on rate for pyCUCU, preventing the full decrease in k_{-2} from appearing in K_d (Tables 1 and 2).

Pulse-Chase Experiments for pyCUCU and L-21 *Sca* I with pG and pdG. The values of k_{-2} were independently determined by pulse-chase experiments (Fig. 4 and Table 1). For pyCUCU, the rate of fluorescence decrease with time, k_{off} , is equal to k_{-2} (16). The values of k_{-2} determined by pulse-chase experiments (Fig. 4) are in agreement with the intercepts in Fig. 3 (Table 1): the rates for pyCUCU dissociation

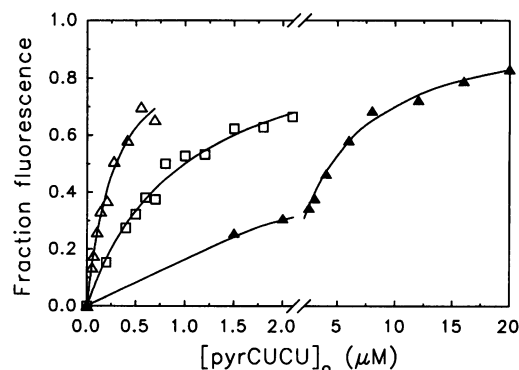


FIG. 2. Equilibrium fluorescence titrations for pyCUCU (pyrCUCU) binding to L-21 *Sca* I with no cofactor (\square), 15 mM pG (\blacktriangle), and 15 mM pdG (\triangle). The solid lines represent the best fits to the data according to a nonlinear least-squares algorithm.

Table 1. Kinetic parameters for 5'-exon mimic binding to L-21 *Sca* I

| Cofactor | Kinetics data with pyCUCU* | | Pulse-chase kinetics data | | | |
|------------------|---|-------------------------------|--|--|---|---|
| | $k_{on} = k_1k_2/k_{-1}$, $\mu\text{M}^{-1}\text{s}^{-1}$ | k_{-2} , s^{-1} | k_{-2} , [†] s^{-1} | Reversed k_{-2} , s^{-1} | Alternate renaturation k_{-2} , s^{-1} | k_{off} with pyCCUCU, s^{-1} |
| None/135 mM NaCl | 0.058 ± 0.002 [‡] | 0.076 ± 0.004 [‡] | 0.075 [‡] | 0.050 | 0.062 | 0.0025 [‡] |
| None/180 mM NaCl | 0.061 ± 0.005 | 0.10 ± 0.01 | 0.083 | | | |
| pG (15 mM) | 0.017 ± 0.001 | 0.099 ± 0.008 | 0.087 | 0.073 | 0.088 | 0.0092 |
| pdG (15 mM) | 0.029 ± 0.002 | 0.0095 ± 0.001 | 0.0090 | 0.012 | 0.0094 | 0.00058 |
| (5 mM) | 0.040 ± 0.002 | 0.0092 ± 0.001 | 0.0069 | | | |
| pA (15 mM) | 0.032 ± 0.003 | 0.086 ± 0.006 | 0.074 | | | |
| pdA (15 mM) | 0.039 ± 0.004 | 0.049 ± 0.004 | 0.056 | | | |

*Kinetic parameters from experiments with pyCUCU at 15°C and 5 mM Mg²⁺ (Fig. 3).

[†]The rate of fluorescence decrease was not affected by 2- to 5-fold higher concentrations of chase oligomer, CUCU, indicating that the rate of pyCUCU dissociation from L-21 *Sca* I is rate-limiting.

[‡]See ref. 16.

in the presence and absence of pG are similar, while the rate when there is saturating pdG is slower by a factor of about 10.

Reversed Pulse-Chase Experiments for pyCUCU and L-21 *Sca* I. To assess the effect of the pyrene fluorophore on the dynamics of binding, rates of dissociation of unlabeled CUCU substrates were determined by reversed pulse-chase experiments (Table 1). Values of k_{-2} for CUCU are similar to those obtained for pyCUCU (Table 1), suggesting that the pyrene fluorophore does not significantly perturb tertiary binding interactions.

Pulse-Chase Experiments for pyCCUCU and L-21 *Sca* I with pG and pdG. Pulse-chase experiments on pyCCUCU binding to L-21 *Sca* I in the absence of a G-like substrate and in the presence of saturating pG or pdG were also conducted. In the case of the pentamer, $k_{off} = k_{-2}k_{-1}/(k_{-1} + k_2)$ (16). The rate of dissociation, k_{off} , for pyCCUCU with pG is 3.7-fold faster than k_{off} for pyCCUCU with no G cofactor (Table 1). Experiments with pyCUCU indicate k_{-2} is insensitive to pG binding. Furthermore, the rate of breaking base pairs between pyCCUCU and L-21 *Sca* I (k_{-1}) is a secondary structure event and unlikely to be affected by occupancy of the G-binding site. Consequently, the following ratio is obtained: $(k_{-1}^{no\ G} + k_2^{no\ G})/(k_{-1}^{pG} + k_2^{pG}) = 3.7$. In the absence of pG, k_2 and k_{-1} are 2.5 and 0.5 s⁻¹ (16), respectively, suggesting a k_2 for pyCCUCU in the presence of pG of 0.3 ± 0.2 s⁻¹. This is roughly 10% the k_2 of 2.5 s⁻¹ measured in the absence of pG. This slower rate of P1 docking for pyCCUCU suggests that the pG-induced slower k_{on} ($= k_1k_2/k_{-1}$) for pyCUCU is due primarily to a slower rate of P1 docking (k_2).

Effect of Alternate Renaturation on Pulse-Chase Experiments. Different renaturation protocols for a circular form of the *T. thermophila* LSU intron lead to different rates for activity (25). To gain insight into whether the properties of

L-21 *Sca* I for substrate binding and cooperativity are sensitive to renaturation protocol, the values of k_{-2} for pyCUCU without the G substrate and with saturating pG and pdG were determined for a second renaturation, similar to the method of Herschlag and Cech (26) (see *Materials and Methods*) (Table 1). Pulse-chase experiments under these conditions gave essentially identical results to those obtained with our renaturation protocol (Table 1) (21). This suggests that the ribozyme is able to fold into a similar structure with both renaturation pathways.

Effect of Ionic Strength on pyCUCU Binding to L-21 *Sca* I. Adding 15 mM pG or pdG to the buffer raises the ionic strength of the buffer by 45 mM. To examine whether the observed changes in binding kinetics and thermodynamics are caused by the increase in ionic strength, two control experiments were performed. In the first experiment, no cofactor was added, but the ionic strength of the buffer was increased 45 mM by raising the concentration of NaCl from 135 to 180 mM. Binding of pyCUCU to L-21 *Sca* I is essentially unchanged by this increase in NaCl (Tables 1 and 2). In the second experiment, the concentration of pdG cofactor added was lowered from 15 to 5 mM. This concentration of pdG should be able to saturate at least 80% of the L-21 *Sca* I (24), yet lowers the increase in ionic strength from 45 to 15 mM. Binding of pyCUCU to L-21 *Sca* I is similar in both 5 and 15 mM pdG (Tables 1 and 2). Apparently the coupling of pyCUCU binding with pG or pdG is not a consequence of the increase in ionic strength associated with addition of G cofactors.

Effects of 15 mM pA and 15 mM pdA on pyCUCU Binding to L-21 *Sca* I. To examine whether the effects of pG and pdG on pyCUCU binding are specific to G monomers only, binding of pyCUCU to L-21 *Sca* I was studied in 15 mM pA

Table 2. Thermodynamic parameters for pyCUCU binding to L-21 *Sca* I

| Cofactor | From titration | | From kinetics | |
|------------------|--------------------------|--|--|--|
| | K_d , μM | $-\Delta G_{T5}^*$, kcal·mol ⁻¹ | $-\Delta G_{T5}^\dagger$, kcal·mol ⁻¹ | $\Delta\Delta G_{T5}^\ddagger$, kcal·mol ⁻¹ |
| None/135 mM NaCl | 0.99 ± 0.13 [§] | 7.9 ± 0.08 [§] | 7.8 ± 0.04 [§] | |
| None/180 mM NaCl | | | 7.6 ± 0.07 | 0.1 ± 0.08 |
| pG (15 mM) | 3.9 ± 0.25 | 7.1 ± 0.04 | 6.9 ± 0.06 | 0.9 ± 0.07 |
| pdG (15 mM) | 0.24 ± 0.083 | 8.7 ± 0.2 | 8.6 ± 0.09 | -0.8 ± 0.1 |
| (5 mM) | | | 8.7 ± 0.07 | -1.0 ± 0.08 |
| pA (15 mM) | | | 7.3 ± 0.07 | 0.4 ± 0.08 |
| pdA (15 mM) | | | 7.8 ± 0.07 | 0.0 ± 0.08 |

* $\Delta G_{T5}^* = RT \ln K_d$, where $R = 0.001987$ kcal·K⁻¹·mol⁻¹, $T = 288.15$ K (15°C), and K_d is the dissociation constant for pyCUCU obtained by titration (Fig. 2).

[†] $\Delta G_{T5}^\dagger = RT \ln [k_{-2}/(k_1k_2/k_{-1})]$, where k_1 , k_{-1} , k_2 , and k_{-2} are the rate constants obtained from kinetics experiments.

[‡] $\Delta\Delta G_{T5}^\ddagger = \Delta G_{T5}^\dagger$ (+ cofactor) - ΔG_{T5}^\dagger (no cofactor), with ΔG_{T5}^\dagger data obtained from kinetics experiments.

[§]See ref. 16.

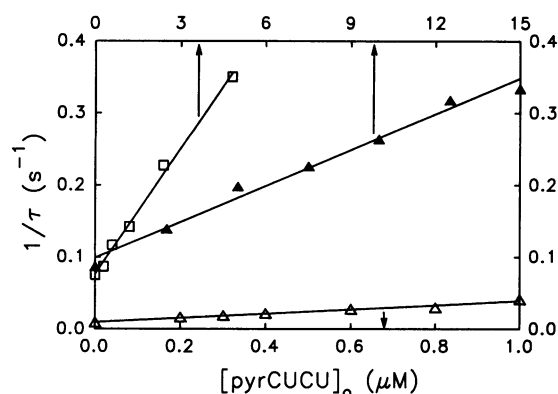


FIG. 3. Dependence of the rate of fluorescence increase with time ($1/\tau$) on the initial pyCUCU (pyrCUCU) concentration for pyCUCU binding to L-21 *Sca* I with no cofactor (\square), 15 mM pG (\blacktriangle), and 15 mM pdG (\triangle). Data points on the ordinate were directly obtained by pulse-chase experiments (Table 1) (Fig. 4). (The y intercept is k_{-2} .) All other data points come from the results of kinetics experiments between pyCUCU and L-21 *Sca* I. The solid lines represent the best fits to the data by a linear least-squares method. Note that experiments with no cofactor and pG use a different concentration axis than experiments with pdG.

and 15 mM pdA. The ΔG_{15}^{\ddagger} for pyCUCU binding to L-21 *Sca* I in the presence of 15 mM pA is intermediate between the ΔG_{15}^{\ddagger} for pyCUCU binding in the absence of any cofactor and in the presence of pG (Table 2). As with pG, the rate of pyCUCU association with L-21 *Sca* I, $k_{\text{on}} = k_1 k_2 / k_{-1}$, is decreased by 15 mM pA, while k_{-2} is almost unchanged (Table 1).

The ΔG_{15}^{\ddagger} for pyCUCU binding to L-21 *Sca* I in the presence of 15 mM pdA is the same as when no cofactor is present (Table 2). However, both k_{on} and k_{-2} are decreased by $\approx 35\%$ by 15 mM pdA (Table 1). These observations suggest that pA and pdA can promote some of the anticooperative and cooperative effects seen with pG and pdG. This observation is consistent with that of Yarus *et al.* that ATP binds to the G-binding site of precursor rRNA for *T. thermophila* at 55°C and 10 mM Mg^{2+} with a K_i of ≈ 8 mM (27). These observations suggest that at least a portion of the coupling interactions between pyCUCU and pG/pdG are due to the sugar.

DISCUSSION

The effects of pG and pdG on the binding of pyCUCU to the catalytic RNA from *T. thermophila* are reported in Tables 1

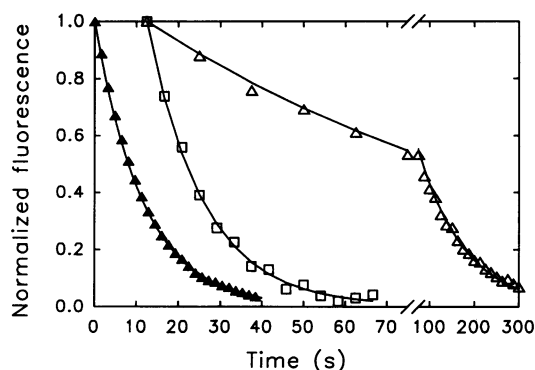


FIG. 4. Dependence of fluorescence decrease on time for pyCUCU dissociating from L-21 *Sca* I from pulse-chase experiments with no cofactor (\square), 15 mM pG (\blacktriangle), and 15 mM pdG (\triangle). The solid lines represent the best single-exponential fits to the data by a nonlinear least-squares method.

and 2. The results indicate that pG has an anticooperative effect, weakening binding of pyCUCU to L-21 *Sca* I by 0.9 kcal/mol, while pdG has a cooperative effect, enhancing binding of pyCUCU to L-21 *Sca* I by -0.8 kcal/mol. This suggests that the packing of the catalytic core is sensitive to the 2'-OH group of the G cofactor.

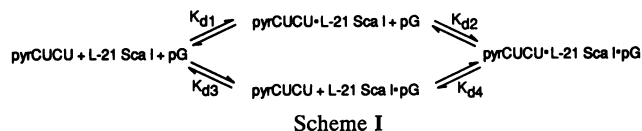
Previous experiments aimed at examining interaction between the two binding sites provide no evidence for coupling of substrate binding to the L-21 *Sca* I ribozyme (26, 28). Kinetic experiments with $\text{G}_2\text{C}_3\text{UCU}$ or $\text{G}_2\text{C}_3\text{UCUA}_5$ provide evidence for random and independent binding of G with each of these substrates at 50°C and 10 mM Mg^{2+} (26). Under conditions used in those experiments, $k_{\text{on}} = k_1$ and $k_{\text{off}} = k_{-1}k_{-2}/k_2$ (15, 16, 26). Results for $\text{G}_2\text{C}_3\text{UCUA}_5$ were interpreted as consistent with the absence of an effect of G on k_{on} and k_{off} (26). However, error limits on k_{off} were assessed to be a factor of 3 or -0.7 kcal/mol at 50°C (26), similar to the magnitude of the effect observed here. Gel shift experiments at 25°C and 42°C and 10 mM Mg^{2+} in the absence and presence of 500 μM G suggested neither C_3UCU nor CUCUCU binding is coupled to G binding (28). While 25°C is close to the 15°C temperature of the experiments reported here, equilibrium dialysis experiments suggest that the K_d values measured by gel retardation at 25°C are not reliable (21). Moreover, 500 μM G is not sufficient to saturate the binding site (24). Thus, while previously reported experiments provide no evidence for coupling between binding of substrates, they do not contradict results reported here.

The possibility of cooperative interactions between the 5'-exon binding site and the G binding site was initially suggested by a comparison of equilibrium dialysis experiments in the presence of pdG and kinetics experiments in the absence of pdG (16, 21). Equilibrium dialysis experiments between ^{32}P -labeled CUCU and fully active L-21 *Sca* I in 5 mM Mg^{2+} in the presence of 5 mM pdG indicate that the ΔG_{15}^{\ddagger} for the second step of CUCU binding to L-21 *Sca* I is -3.8 kcal/mol (21). Stopped-flow experiments between pyCUCU and L-21 *Sca* I in 5 mM Mg^{2+} with no G cofactor indicate that the ΔG_{15}^{\ddagger} for the second step of pyCUCU binding to L-21 *Sca* I is only -2.4 kcal/mol (16). This suggested that pdG enhances binding of CUCU by approximately -1.4 kcal/mol (16). Experiments reported here confirm that pdG is responsible for about half of this additional free energy.

Kinetics experiments indicate that the anticooperative and cooperative effects of pG and pdG appear primarily in the second step of pyCUCU binding to L-21 *Sca* I—i.e., in formation and disruption of tertiary structure. Although the G- and pyCUCU-binding sites are ≈ 235 nucleotides apart in the secondary structure (18, 19, 29, 30), they must come within several angstroms of each other in the tertiary structure to facilitate reaction (31, 32). Consequently, the observation that the interaction between the two sites occurs upon formation of tertiary structure between the P1 duplex and the catalytic core is reasonable. In the presence of pG, weaker binding of pyCUCU to L-21 *Sca* I occurs primarily because of a slower k_2 , the rate of forming tertiary contacts between P1 and the catalytic core (Fig. 1). This effect could have several origins. For example, binding of pG may induce a conformational change of the ribozyme's catalytic core that sterically hinders P1 access to the core, or the core may have greater preorganization favorable to P1 docking in the absence of pG. In the presence of pdG, stronger binding of pyCUCU to L-21 *Sca* I occurs primarily because of a slower k_{-2} , the rate of breaking tertiary contacts between P1 and the catalytic core (Fig. 1). This suggests that binding of pdG either permits an additional tertiary contact to be made in the termolecular pyCUCU-L-21 *Sca* I-pdG complex, or alternatively, that binding of pdG prohibits an unfavorable contact from being made in the termolecular complex. The difference of 1.7 kcal/mol between binding in the presence of pG and

pdG shows that the ribozyme can discriminate between a 2'-OH and a 2'-H. Thus, small structural changes can lead to large changes in individual rates.

The results for binding of pyCUCU in the presence and absence of pG and pdG also have implications for the binding of pG and pdG in the presence and absence of pyCUCU. The equilibria involved in formation of the termolecular pyCUCU-L-21 *Sca I*-pG complex are shown in Scheme I:



The results in Table 2 show that $K_{d1} < K_{d4}$ in the presence of saturating pG and $K_{d1} > K_{d4}$ in the presence of saturating pdG. From Scheme I, $K_d = K_{d1}K_{d2} = K_{d3}K_{d4}$. Thus, in the presence of saturating pyCUCU, $K_{d3} < K_{d2}$ for pG and $K_{d3} > K_{d2}$ for pdG. That is, pG should bind more weakly in the presence than in the absence of pyCUCU. The reverse should be true for pdG.

Fluorescent dyes provide a convenient means of visualizing local dynamics in a large system. However, one concern is that the dye may perturb various interactions. Reversed pulse-chase experiments indicate that the dissociation of unlabeled CUCU from L-21 *Sca I* is similar to dissociation of pyCUCU both in the absence of a G cofactor and in the presence of either pG or pdG (Table 1). Other experiments also indicate that the pyrene is nonperturbing (16, 17). Energy minimization and molecular dynamics calculations suggest that pyrene may be located in the major groove of the P1 duplex (17). This would allow the 2'-OH groups in the minor groove of a P1 helix formed with pyCUCU to make proper tertiary contacts with the catalytic core.

The comparisons between pyCUCU binding to L-21 *Sca I* with the G-binding site occupied by pG or pdG indicate that the two binding sites are able to communicate with one another. The interaction energies between pyCUCU and pG or pdG of ≈ 1 kcal/mol are similar to those observed in cooperative protein enzymes (22). The presence of cooperative effects represents a possible means for *T. thermophila* to regulate its splicing in response to local G and dG concentrations. Perhaps the cooperative substrate interactions in the ribozyme reflect early steps towards the evolution of regulatory enzymes.

1. Wyman, J. (1964) *Adv. Protein Chem.* 19, 223-286.

2. Monod, J., Wyman, J. & Changeux, J. P. (1965) *J. Mol. Biol.* 12, 88-118.

3. Koshland, D. L., Jr., Nemethy, G. & Filmer, D. (1966) *Biochemistry* 5, 365-385.

4. Ackers, G. (1979) *Biochemistry* 18, 3372-3380.

5. Bohr, C. (1903) *Zentralbl. Physiol.* 17, 682.

6. Benesch, R. & Benesch, R. E. (1967) *Biochem. Biophys. Res. Commun.* 26, 162-164.

7. Mildvan, A. (1972) *Biochemistry* 11, 2819-2828.

8. Van Schaftingen, E., Hue, L. & Hers, H. G. (1980) *Biochem. J.* 192, 897-901.

9. Helmreich, E. & Cori, C. F. (1964) *Proc. Natl. Acad. Sci. USA* 51, 131-138.

10. Jacobson, G. R. & Stark, G. R. (1973) in *Enzymes*, 3rd Ed. 9, 225-308.

11. Thelander, L. & Reichard, P. (1979) *Annu. Rev. Biochem.* 48, 133-158.

12. Gilman, A. G. (1987) *Annu. Rev. Biochem.* 56, 615-649.

13. Zaug, A. J., Grosshans, C. A. & Cech, T. R. (1988) *Biochemistry* 27, 8924-8930.

14. Bass, B. L. & Cech, T. R. (1986) *Biochemistry* 25, 4473-4477.

15. Herschlag, D. H. (1992) *Biochemistry* 31, 1386-1399.

16. Bevilacqua, P. C., Kierzek, R., Johnson, K. A. & Turner, D. H. (1992) *Science* 258, 1355-1358.

17. Kierzek, R., Li, Y., Turner, D. H. & Bevilacqua, P. C. (1993) *J. Am. Chem. Soc.* 115, 4985-4992.

18. Davies, R. W., Waring, R. B., Ray, J. A., Brown, T. A. & Scazzocchio, C. (1982) *Nature (London)* 300, 719-724.

19. Been, M. D. & Cech, T. R. (1986) *Cell* 47, 207-216.

20. Pyle, A. M. & Cech, T. R. (1991) *Nature (London)* 350, 628-631.

21. Bevilacqua, P. C. & Turner, D. H. (1991) *Biochemistry* 30, 10632-10640.

22. Weber, G. (1975) *Adv. Protein Chem.* 29, 1-83.

23. Johnson, K. (1986) *Methods Enzymol.* 134, 677-705.

24. Moran, S., Kierzek, R. & Turner, D. H. (1993) *Biochemistry* 32, 5247-5256.

25. Walstrum, S. A. & Uhlenbeck, O. C. (1991) *Biochemistry* 29, 10573-10576.

26. Herschlag, D. H. & Cech, T. R. (1990) *Biochemistry* 29, 10159-10171.

27. Yarus, M., Illangesekare, M. & Christian, E. (1991) *Nucleic Acids Res.* 19, 1297-1304.

28. Pyle, A. M., McSwiggen, J. A. & Cech, T. R. (1990) *Proc. Natl. Acad. Sci. USA* 87, 8187-8191.

29. Michel, F., Hanna, M., Green, R., Bartel, D. P. & Szostak, J. W. (1989) *Nature (London)* 342, 391-395.

30. Burke, J. M., Esherrick, J. S., Burfeind, W. R. & King, J. L. (1990) *Nature (London)* 344, 80-81.

31. Michel, F. & Westhof, E. (1990) *J. Mol. Biol.* 216, 585-610.

32. Kim, S.-H. & Cech, T. R. (1987) *Proc. Natl. Acad. Sci. USA* 84, 8788-8792.

33. Inoue, T. & Kay, P. S. (1987) *Nature (London)* 327, 343-346.